

Supported and mixed oxide catalysts based on iron and titanium for the oxidative decomposition of chlorobenzene

Abbas Khaleel*, Aysha Al-Nayli

Department of Chemistry, UAE University, Al-Ain 17551, United Arab Emirates

Received 5 April 2007; received in revised form 5 October 2007; accepted 27 November 2007

Available online 3 December 2007

Abstract

Iron oxide supported on titanium dioxide ($\text{Fe}_2\text{O}_3/\text{TiO}_2$) and iron–titanium mixed oxide (Fe–Ti-oxide) catalysts were prepared via wetness impregnation and sol–gel methods, respectively. The catalytic activity of the two materials for the oxidation of chlorobenzene was studied and compared with the activity of pure titanium and iron oxides as well as MgO-supported iron oxide. $\text{Fe}_2\text{O}_3/\text{TiO}_2$ and Fe–Ti-oxide have shown higher catalytic activities for the oxidation of chlorobenzene than the corresponding pure iron and titanium oxides at a reaction temperature of 325 °C, and this enhanced activity was more pronounced at higher temperatures. The Fe–Ti-oxide, in particular, exhibited a unique activity for the complete oxidation at relatively low temperature, 325 °C, without the formation of other chlorinated organics. Chlorine, measured by iodometric titration was the only Cl-containing product. The absence of HCl as a product and the negative effect of water suggest that the surface active sites are more likely to be Lewis acid–base sites on which chlorobenzene molecules dissociatively adsorb forming metal–Cl bonds and surface phenolate intermediates. Desorption of Cl_2 from the surface and possible interaction of the aromatic ring with metal sites result in the activation of the ring forming partially oxidized intermediates involving lattice oxygen ions. Finally, reactions with molecular oxygen result in the complete oxidation to CO_2 and regenerate the surface.

© 2007 Elsevier B.V. All rights reserved.

Keywords: Chlorobenzene; Catalytic oxidation; Iron–titanium oxides

1. Introduction

Chlorinated organic compounds (COCs) have been always considered among the most hazardous organics that are emitted into the environment. Besides their direct hazardous effects on human health, they are considered among the substances that result in the depletion of the stratospheric ozone layer. As a result of their widely spread applications, their production and hence their emission into the environment is rapidly increasing. Therefore, the decomposition and removal of these pollutants has been always a subject of great importance. Chlorobenzenes are usually studied as model molecules for the more hazardous PCDDs and they are believed to be intermediates for their formation [1].

The most commonly employed process for chemical waste treatment on large scale is incineration, which typically

requires high temperatures to achieve complete combustion. Chlorinated aromatic compounds, as an example, require temperatures between 800 and 1000 °C. Besides the high costs, due to high temperatures, the incineration process is always associated with the formation of a wide range of toxic byproducts such as NO_x , dioxins and dibenzofurans. The methods commonly employed in removing gaseous pollutants from industrial gas streams include wet scrubbing and adsorption. While these methods are relatively efficient in removing several gaseous pollutants, their efficiency towards COCs is very limited [2].

Catalytic oxidation of COCs to CO_2 , HCl, and H_2O using metal or transition metal oxide catalysts has been the most promising alternative. This method requires relatively lower temperatures, shows higher efficiencies, and ensures lower selectivity to harmful byproducts. Generally, supported noble metal catalysts exhibit higher catalytic activities as compared with metal oxide catalysts. However, disadvantages of noble metals, compared with metal oxides, include: (a) their higher costs, (b) deactivation due to their sensitivity to poisons,

* Corresponding author. Tel.: +971 37134065; fax: +971 37671291.

E-mail address: abbask@uaeu.ac.ae (A. Khaleel).

especially in the presence of chlorine atoms and (c) sintering at higher temperatures [3]. On the other hand, transition metal oxide catalysts have several advantages including higher thermal stability, lower costs, and the possibility of fabrication in high-surface area porous powders. Therefore, transition metal oxides have been studied extensively as appropriate catalysts for the total combustion of chlorinated organics [2,4]. While VO_x -based materials are the most widely used catalytic systems [5,6], other catalysts that have shown significant activity include AMnO_3 perovskites (A represents lanthanide ions) [7], and Cr_2O_3 - as well as Fe_2O_3 -based catalysts [8] although chromium oxide-based catalysts have shown some deactivation in the presence of Cl_2 [9].

This paper presents the results of a study on the activity of several Fe_2O_3 - and TiO_2 -based catalysts for the total oxidation of chlorobenzene. Pure oxides are compared with supported and mixed oxide catalysts. FTIR spectroscopy was used for qualitative as well as quantitative probing of the catalytic reactions.

2. Experimental methodology

2.1. Materials and characterization

Chlorobenzene (99.9% pure), iron(III) nitrate nonahydrate (98%), titanium(IV) *n*-butoxide (97%), and 2-propanol (99.7%) were purchased from Aldrich and used as received. Distilled deionized water was used in all reactions. TiO_2 (44 m^2/g , anatase) was obtained from Degussa. Nanostructured iron oxide (nano- α - Fe_2O_3 , 172 m^2/g) was purchased from MACH I Incorporation. MgO (340 m^2/g) was prepared through sol-gel method according to a published procedure [10] except that the solvent was removed from the gel in a water bath at 65 °C resulting in $\text{Mg}(\text{OH})_2$ powder which was then converted to MgO by calcinations at 500 °C for 6 h. $\text{Fe}_2\text{O}_3/\text{MgO}$ (158 m^2/g) was prepared by adsorption of iron(III) acetylacetonate from THF solution according to a procedure published elsewhere [11].

TiO_2 -supported Fe_2O_3 , $\text{Fe}_2\text{O}_3/\text{TiO}_2$ with 4% loading of iron oxide was prepared by incipient wetness impregnation. The iron precursor was $\text{Fe}(\text{NO}_3)_3 \cdot 9\text{H}_2\text{O}$ and TiO_2 (Degussa) was used as the support. The impregnated samples were dried in air at 120 °C for 3 h and then calcined at 500 °C for 5 h.

Fe-Ti mixed oxide, Fe-Ti-oxide, with Fe:Ti molar ratio of 1:1 was prepared by sol-gel method using titanium(IV) *n*-butoxide, $\text{Ti}(\text{O}i\text{Bu})_4$ and $\text{Fe}(\text{NO}_3)_3 \cdot 9\text{H}_2\text{O}$. In a typical experiment, 3.0 mL (8.8×10^{-3} mol) of $\text{Ti}(\text{O}i\text{Bu})_4$ was dissolved in 20 mL 2-propanol and 3.55 g of $\text{Fe}(\text{NO}_3)_3 \cdot 9\text{H}_2\text{O}$ was separately dissolved in 50 mL of the same solvent. While stirring, the iron nitrate solution was added to the titanium butoxide solution followed by dropwise addition of 0.7 mL H_2O . The mixture was stirred for 7 h and aged for 12 more hours giving a brown gel. The solvent was removed by evaporation in a water bath at 70 °C and the obtained red-brown solid was further dried in an oven at 120 °C for 4 h. Calcination at 400 °C for 5 h resulted in a black powder having a specific surface area of 206 m^2/g .

The catalysts were characterized by powder X-ray diffraction (XRD) and N_2 adsorption. Powder X-ray diffraction (XRD) analyses were obtained using a Philips PW/1840 diffractometer with Cu $\text{K}\alpha$ radiation, $\lambda = 1.542 \text{ \AA}$. BET surface area measurements were obtained using nitrogen gas adsorption at 77 K employing a Quantochrome Autosorb-1 volumetric gas sorption instrument. All samples were pretreated at 120 °C under vacuum for 20 min prior to each measurement.

2.2. FTIR study of the gaseous products of the catalytic reactions

The catalytic reactions were studied using a pulse-flow reactor coupled with an FTIR spectrophotometer (Nicolet Nexus 470). An IR cell was connected directly to the reactor allowing for in situ analysis of the gaseous products exiting the reactor. The IR cell was made of a 10-cm long Pyrex tube (25-mm diameter) equipped with two KBr windows and an inlet and outlet for gases. The reactor was a stainless steel U-shaped tube of 4 mm inside diameter. The inlet gas stream contained 1.2 vol.% chlorobenzene and 25% O_2 diluted in He to obtain 20 mL/min. In all experiments 0.15 g of the catalyst (120–180 mesh particles) was packed in the reactor between glass wool plugs. Before each reaction, the catalyst was heated for 1 h in the same He/ O_2 flow at 400 °C, except for the pure iron oxide which was treated at 300 °C. The reactor was heated using a tube furnace and the temperature was monitored by a temperature controller equipped with a K-type thermocouple positioned in the proximity of the catalyst bed. Chlorobenzene was introduced as 1 μL (9.8×10^{-3} mmol) pulses in the inlet stream through a heated injection port positioned just before the reactor where it immediately evaporates. The gases exiting the reactor were allowed to flow through the gas IR cell which was connected directly to the reactor and placed in the FTIR spectrometer chamber. The line beyond the reactor, including the IR cell, was heated at 150 °C using heating tapes to avoid any condensation. FTIR spectra of the products were recorded continuously every 15 s starting immediately after each pulse. Recording spectra was stopped after a steady-state condition was reached where no gases were observed in the spectra. A spectrum of the cell with flowing He/ O_2 gas, recorded separately under the same conditions without a reaction, was subtracted as a background from each spectrum. The % conversion was calculated based on the area of the peak representing $\nu_{\text{C-Cl}}$ of chlorobenzene at 740 cm^{-1} using the ratio of the peak area in the spectrum of the products to the corresponding peak area in a spectrum collected in a blank experiment carried out under the same conditions without the presence of any catalyst.

In addition to the FTIR identification of the products, Cl_2 was measured by iodometric titration. The eluting gas stream was allowed to bubble in a trap containing 3.0 mL of 0.1 M KI aqueous solution where the produced Cl_2 oxidizes the iodide to iodine. The iodine was titrated with 0.05 M aqueous solution of sodium thiosulfate to determine the amount of chlorine.

3. Results and discussion

3.1. Catalysts characterization

The XRD analysis of the supported catalysts, $\text{Fe}_2\text{O}_3/\text{TiO}_2$ and $\text{Fe}_2\text{O}_3/\text{MgO}$ calcined at 500°C showed the typical patterns of the support materials indicating appropriate dispersion of the supported phase and the absence of any crystalline iron oxide. The analysis of $\text{Fe}_2\text{O}_3/\text{TiO}_2$ (Fig. 1) showed the presence of two TiO_2 phases, anatase ($\sim 70\%$) and rutile ($\sim 30\%$) while the starting pure TiO_2 consisted of pure anatase. The specific surface areas of $\text{Fe}_2\text{O}_3/\text{TiO}_2$ and $\text{Fe}_2\text{O}_3/\text{MgO}$ were 41 and $158\text{ m}^2/\text{g}$, respectively.

The XRD analysis (Fig. 2) of the mixed oxide catalyst, Fe–Ti-oxide indicated an amorphous solid after calcination at 500°C . Very weak diffraction pattern was obtained which matched, to a very good degree, the known pattern of $\text{Fe}_2\text{Ti}_3\text{O}_9$ having a pseudorutile structure. The broad peaks at $2\theta = 36^\circ$, 41.3° and 54.3° indicates the pseudorutile phase [12]. The absence of a diffraction peak at 27.3° confirms that these features represent pseudorutile and not rutile phase. There was no evidence for the presence of any crystalline iron oxide or titania pure phases. After heating at 600°C , peaks corresponding to hematite and rutile were observed. The hematite is indicated by the peak at 32.9° and rutile is indicated by the peak at 27.3° which refer to reflections from (1 1 0) plane. Although it is difficult to distinguish the peaks corresponding to pseudorutile from those of rutile, the relatively higher intensity at 41° compared with the one at 27.3° and the intense peak at 54.3° clearly indicate the presence of pseudorutile. More work is undergoing for further textural and structural characterizations of this material.

Interestingly, this material showed surface areas significantly higher and more stable than those of the corresponding supported catalyst and pure oxides. Samples calcined at 400 and 500°C showed specific surface areas of 206 and $127\text{ m}^2/\text{g}$, respectively. As will be discussed later, this decrease in the

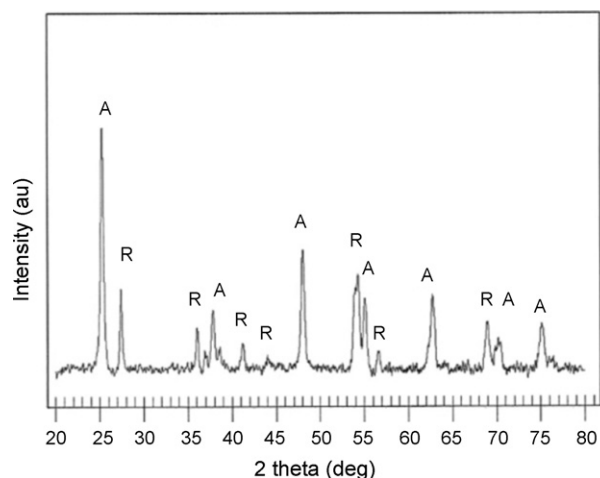


Fig. 1. The XRD analysis of the $\text{Fe}_2\text{O}_3/\text{TiO}_2$ after calcination at 500°C . 'A' and 'R' refer to anatase and rutile, respectively.

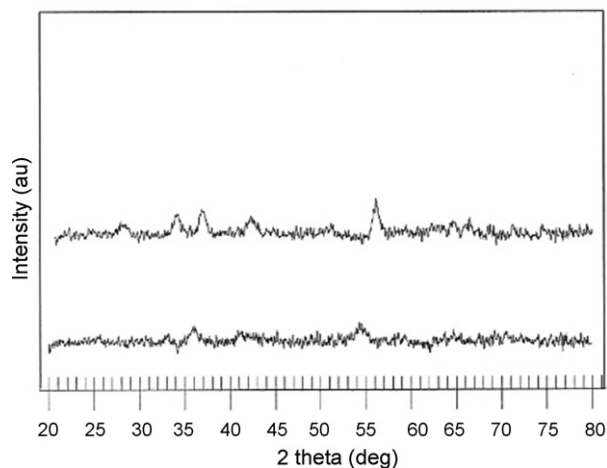


Fig. 2. The XRD analysis of the mixed oxide catalyst, Fe–Ti-oxide after calcination at 500 and 600°C (the top diffractogram).

specific surface area upon heating is relatively less than the corresponding decrease for the pure oxides. This means that combining both metals in a mixed oxide enhanced the stability against sintering and significantly preserved the surface area at elevated temperatures.

3.2. The pulse-flow-FTIR method

The pulse-flow-FTIR was a useful technique for qualitative as well as quantitative evaluation of the catalytic reactions. The products along with any remaining chlorobenzene exited the reactor and the IR cell as a relatively sharp pulse allowing for quantitative measurement of the unreacted chlorobenzene. The shape of the chlorobenzene pulse after it passes through the reactor is plotted in Fig. 3. While unreacted chlorobenzene always exited the catalyst bed and the IR cell as a relatively sharp pulse, the CO_2 product, in some cases, continued to desorb more gradually indicating continuous formation from different types of surface intermediates. About 2 min after each

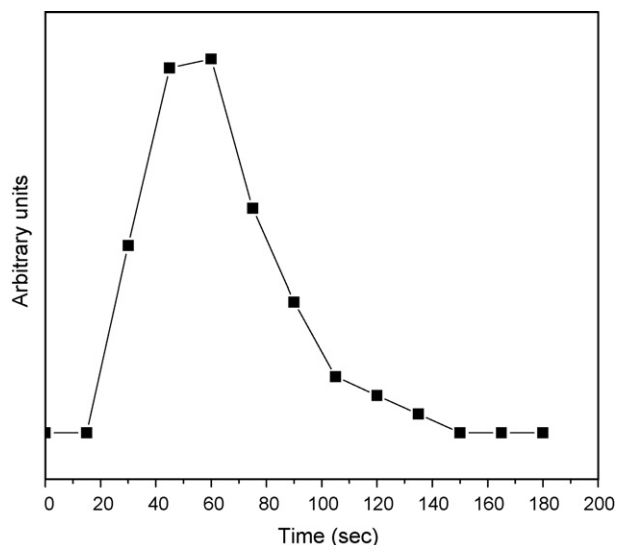


Fig. 3. The shape of a chlorobenzene pulse as it passes through the IR cell.

pulse, the gas phase returned to its initial equilibrium where no peaks were observed in the spectra. The fourth and the fifth spectra from each pulse represented the full amount of chlorobenzene exiting the reactor and were used for the quantitative evaluation of the conversion. In addition, this technique allows for observing different stages of products' evolution from one pulse.

An example of typical results is presented in Fig. 4, which shows the FTIR spectra of the gaseous products from different pulses over $\text{Fe}_2\text{O}_3/\text{TiO}_2$ catalyst at 325 °C. Each spectrum, which represents a pulse, clearly identifies the remaining chlorobenzene and the IR-active products. The absence of HCl as a product is indicated by the absence of the peaks representing HCl between 2750 and 3100 cm^{-1} .

3.3. The catalytic activity of the pure oxides, Fe_2O_3 , TiO_2 and MgO

The catalytic activities of the pure oxides were compared at 325 °C in experiments involving 40 1- μL pulses. Although MgO has the highest surface area among them, it exhibited the lowest catalytic activity as shown in Fig. 5. This is what one may expect since MgO is a very ionic oxide compared with the transition metal oxides where the lattice oxygen is relatively more labile and can be involved in oxidation–reduction reactions. Besides, the low activity and the fast deactivation of MgO could be, in part due to its possible chlorination in the presence of Cl_2 or other Cl-containing species. Nano- $\alpha\text{-Fe}_2\text{O}_3$ exhibited higher catalytic activity than TiO_2 especially in the beginning, over fresh samples, where the first three pulses were completely decomposed before a break-through of chlorobenzene was observed. On the other hand, TiO_2 showed only 70% conversion in the first two pulses which then declined gradually to less than 30%. The catalytic activity of the nano- $\alpha\text{-Fe}_2\text{O}_3$ was also compared with that of its low-surface area (LSA- $\alpha\text{-Fe}_2\text{O}_3$) counterpart, obtained from Aldrich, having a specific surface area of 4.2 m^2/g . The LSA- $\alpha\text{-Fe}_2\text{O}_3$ showed considerably lower conversion than its high-surface area analogue. While the first three pulses were completely decomposed over the nano- $\alpha\text{-Fe}_2\text{O}_3$, the low-surface area sample gave only 45% conversion in the first pulse and after 15 pulses, the conversion reached a steady-state condition with conversion less than 25%. The apparent difference in the initial catalytic activity can be referred, in principle, to the difference in surface areas as larger surfaces typically result in larger amount of adsorption. This phenomenon becomes less significant as the surface coverage increases. After sometime (after ~ 10 pulses according to the results in Fig. 5) the difference in the actual activities is observed.

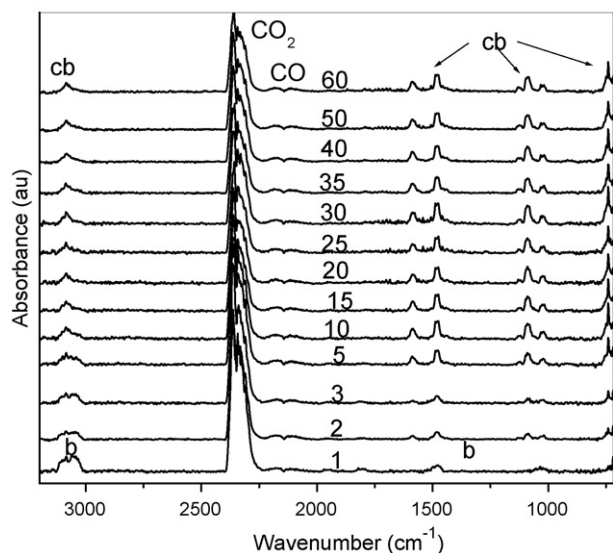


Fig. 4. FTIR spectra of the gaseous products of chlorobenzene oxidation over $\text{Fe}_2\text{O}_3/\text{TiO}_2$ at 325 °C. The letters 'b' and 'cb' refer to benzene and chlorobenzene, respectively. The numbers 1–60 represent the pulse number.

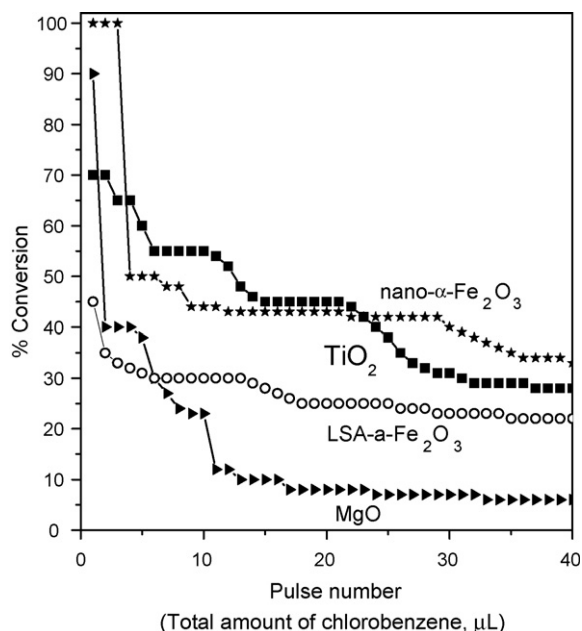


Fig. 5. The conversion of chlorobenzene over the pure oxide catalysts at 325 °C.

The catalytic activity exhibited by pure iron oxide is interesting since it can be prepared by cost-effective methods [13] and can be commercially obtained in relatively high-surface areas. Besides, iron is the most abundant metal and its oxides do not create significant disposal problems. Therefore, nano- $\alpha\text{-Fe}_2\text{O}_3$ was studied in more details. The XRD analysis (Fig. 6) of nano- $\alpha\text{-Fe}_2\text{O}_3$ after reactions at 325 °C showed the typical pattern of $\alpha\text{-Fe}_2\text{O}_3$ indicating no phase or composition changes. The surface area dropped considerably from 172 m^2/g before the reaction to 28 m^2/g after the reaction which most likely caused the rapid decrease in its catalytic activity. The considerable sintering, and hence loss of surface area of the nano- $\alpha\text{-Fe}_2\text{O}_3$ was also observed when the as-purchased material (172 m^2/g) was calcined at 400 °C where the specific surface area dropped to 37 m^2/g .

When the reaction was carried out in the absence of O_2 at 400 °C, nano- $\alpha\text{-Fe}_2\text{O}_3$ showed some oxidation activity with CO_2 as the major product. The conversion was considerably lower than that in the presence of O_2 , as expected, and continued to decline as shown in Fig. 7. The solid turned from

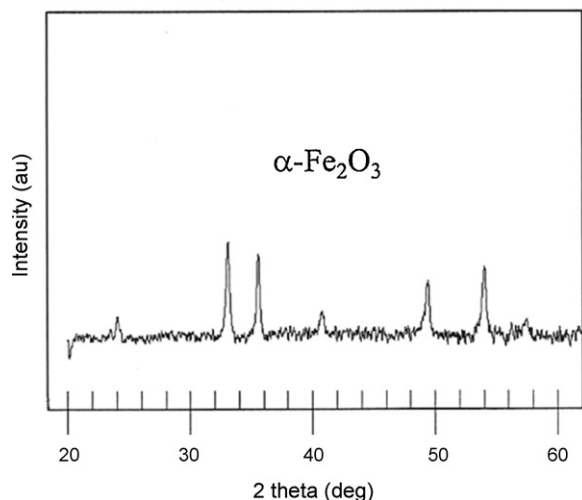


Fig. 6. The XRD analysis of nano- α - Fe_2O_3 after reaction with chlorobenzene at 325 °C in the presence of oxygen.

reddish color, before the reaction, to black after the reaction and was identified by XRD to be pure Fe_3O_4 . This reduction of nano- α - Fe_2O_3 and the oxidation of chlorobenzene in the absence of oxygen strongly suggest that the mechanism in the presence of oxygen probably involves reduction of the surface by abstraction of lattice oxygen. The surface is then regenerated by reaction with gas phase oxygen molecules. This also means that the observed catalytic activity of iron oxide and other iron oxide-based catalysts can be referred to the reducibility of nano- α - Fe_2O_3 . The fact that this reduction was not limited to the surface clearly shows significant small-particle-size effect which allowed for the accessibility of the bulk. This becomes evident when we compare this behavior with that of the LSA- α - Fe_2O_3 in the absence of oxygen, where no such reduction was observed. Only negligible amounts of CO_2 formed and the XRD analysis of the solid after the reaction showed no reduction to Fe_3O_4 indicating that the reaction was limited to the surface.

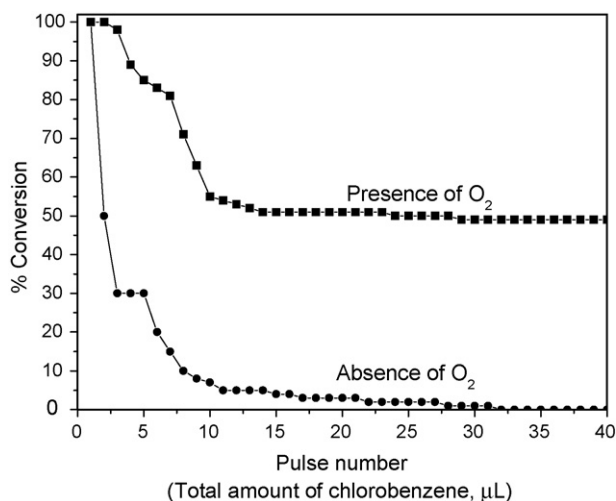


Fig. 7. The conversion of chlorobenzene over nano- α - Fe_2O_3 at 400 °C in the presence and in the absence of oxygen.

3.4. The catalytic activity of the supported catalysts, $\text{Fe}_2\text{O}_3/\text{TiO}_2$ and $\text{Fe}_2\text{O}_3/\text{MgO}$

Interestingly, $\text{Fe}_2\text{O}_3/\text{TiO}_2$ exhibited higher catalytic activity than its pure components, Fe_2O_3 and TiO_2 . In a study at 325 °C involving 60 1- μL pulses, the steady-state conversion using the supported catalyst was around 60% as compared with less than 35% for the pure components as shown in Fig. 8. To point out the effect of the support, the catalytic activity of MgO -supported Fe_2O_3 and $\text{Fe}_2\text{O}_3/\text{MgO}$ was also studied under the same conditions. Although $\text{Fe}_2\text{O}_3/\text{MgO}$ has significantly higher surface area (158 m^2/g) than $\text{Fe}_2\text{O}_3/\text{TiO}_2$ (41 m^2/g), it showed considerably lower catalytic activity indicating a key role of the support. The conversion started with only 95% over the fresh sample and declined rapidly to around 15% (Fig. 8). The enhanced activity exhibited by TiO_2 as a support can be referred to two reasons. First, the better ability of titania to disperse iron oxide on the surface which is supported by similar literature reports where titania has been reported to result in better spreading of several active phase transition metal oxides compared with alumina and silica [14]. Second, chlorobenzene is known to adsorb on the acidic surface of TiO_2 while it does not adsorb significantly on the basic MgO surface. Besides these two reasons, the activity of the $\text{Fe}_2\text{O}_3/\text{TiO}_2$ catalyst is enhanced by some type of synergic interaction between surface iron oxide and the support, TiO_2 . This became evident from a similar activity study on Fe–Ti mixed oxide catalyst as will be discussed in the next section.

The products detected by FTIR include CO_2 , C_6H_6 , H_2O , and negligible traces of CO . Surprisingly, no HCl was observed and Cl_2 was the only Cl-containing product as determined by the iodometric titration. The absence of $\nu_{\text{C-Cl}}$ absorption bands, other than the typical bands of chlorobenzene, in the region of

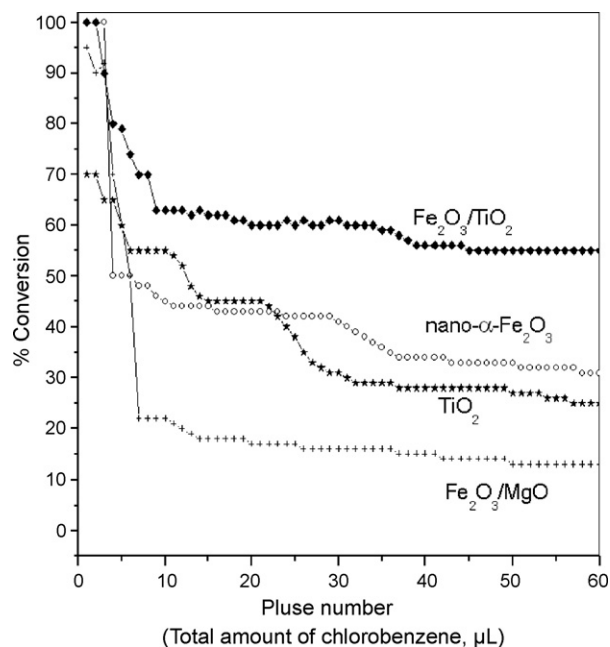


Fig. 8. The conversion of chlorobenzene over $\text{Fe}_2\text{O}_3/\text{TiO}_2$ compared with its pure components and $\text{Fe}_2\text{O}_3/\text{MgO}$ at 325 °C.

400–900 cm^{-1} indicates the absence of any chlorinated hydrocarbon products including polychlorinated benzene. One observation that is worth pointing out is that in all pulses with 100% conversion, whether in the case of pure Fe_2O_3 or $\text{Fe}_2\text{O}_3/\text{TiO}_2$, some benzene formed while it was not observed from any of the pulses associated with partial conversion. This indicates that the reactions on the fresh surface involve two different processes. The first one involves C–Cl bond cleavage only allowing for desorption of benzene molecules, and the other process involves the C–Cl bond cleavage and the oxidation of the benzene ring. It is possible that the first process takes place on specific sites on the fresh surface and that these sites get blocked as the reaction goes on. Therefore, as these sites are deactivated, the formation of benzene ceases. Another way to explain this phenomenon is that the fresh surfaces result in high concentration of adsorbed Cl atoms and benzene molecules. The high concentration of adsorbed benzene allows for some desorption before further oxidation. On the other hand, lower conversion results in lower concentration of adsorbed benzene intermediate allowing for further interaction with the surface and activation, especially after desorption of the adsorbed Cl atoms from the surface.

In some experiments, the reaction at 325 °C was stopped after the steady-state condition was reached (around 60% conversion) and the sample was heated at 350 °C for 1 h in the He/O_2 flow before resuming the reaction. It was found that the sample gained its initial activity and acted, to a very good extent, as the fresh sample. The first two pulses after the perturbation were completely oxidized before going back to a steady-state condition similar to that before the perturbation. These results clearly indicate that one reason of the deactivation of the catalyst is the rapid accumulation of adsorbed residues on the surface. The further heat treatment at slightly higher temperature resulted in the removal of such residues regenerating the active surface. Reactions studied at higher temperatures, discussed below, further support this suggestion where higher conversions were obtained at elevated reaction temperatures.

At higher reaction temperatures, 350 and 400 °C, $\text{Fe}_2\text{O}_3/\text{TiO}_2$ exhibited higher catalytic activities compared with that at 325 °C. In a study involving 100 pulses, a reaction temperature of 350 °C resulted in complete conversion during the first 10 pulses before reaching a steady-state condition with about 85–90% conversion as shown in Fig. 9. At 400 °C the catalyst showed significantly higher activity where continuous 100% conversion was obtained. Besides the higher conversion, less benzene and CO were observed at 400 °C as compared with lower temperatures indicating an enhanced deep oxidation of the aromatic ring to CO_2 . The catalyst retained its ability for 100% conversion when the size of the chlorobenzene pulse was doubled to 2 μL , while introducing 3 μL pulses resulted in about 80% conversion. The formation of benzene was also tested at elevated reaction temperatures, 425–600 °C. Although 100% conversion was obtained, benzene continued to form at temperatures as high as 550 °C, and it completely ceased at 575 °C where complete oxidation was observed.

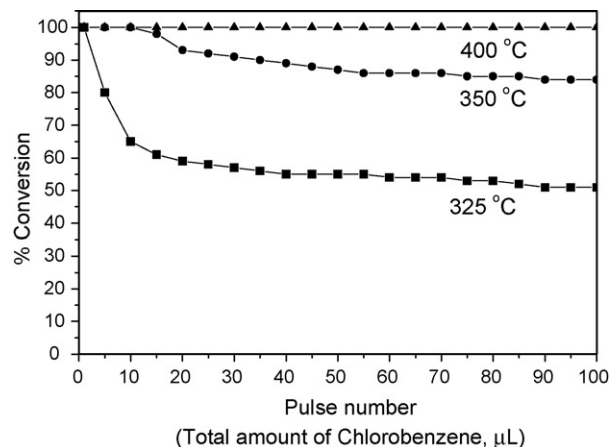


Fig. 9. The conversion of chlorobenzene over $\text{Fe}_2\text{O}_3/\text{TiO}_2$ at different temperatures.

The powder XRD analysis of $\text{Fe}_2\text{O}_3/\text{TiO}_2$ after reactions at 325 °C showed no phase changes. After reactions at 400 °C, no changes were also observed except some anatase transformation to rutile. The catalyst before reactions (calcined at 500 °C) showed a mixture of anatase (70%) and rutile (30%) phases. After the reaction at 400 °C, it showed a 1:1 mixture of both phases.

The difference in the catalytic activity between $\text{Fe}_2\text{O}_3/\text{TiO}_2$ and its pure components was more pronounced at 400 °C as shown in Fig. 10. The temperature increase from 325 to 400 °C resulted in only slight increase in the activity of the pure oxides while significantly enhanced the activity of the supported catalyst (compare Figs. 10 and 8). These variations are possibly due to the higher ability of the supported catalyst to retain its specific surface area (Table 1) upon heating as compared with the pure iron oxide, which clearly plays a major role in the process over the supported catalyst. As one may expect, high-surface area corresponds to larger amounts of adsorption and higher temperatures enhance the mobility of the surface oxygen and hence enhance the oxidation–reduction process.

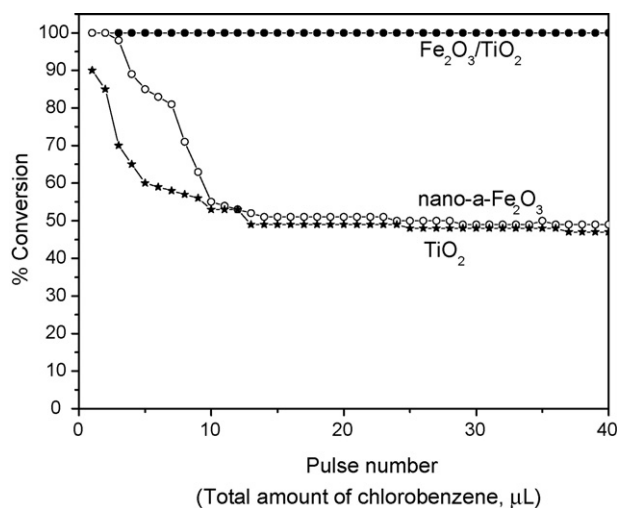


Fig. 10. The conversion of chlorobenzene at 400 °C by $\text{Fe}_2\text{O}_3/\text{TiO}_2$ and its pure components, Fe_2O_3 and TiO_2 .

Table 1

The specific surface areas (m^2/g) of the titanium and iron oxide catalysts after calcination at different temperatures and before and after reactions at 325°C

	After calcination			Before reaction	After reaction
	300 $^\circ\text{C}$	400 $^\circ\text{C}$	500 $^\circ\text{C}$		
TiO_2	–	–	44	44	39
Nano- α - Fe_2O_3	172	37	24	172	28
$\text{Fe}_2\text{O}_3/\text{TiO}_2$	–	–	41	41	39
Fe–Ti-oxide	–	206	137	206	105

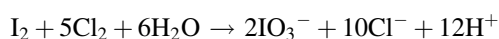
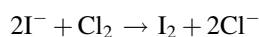
3.5. The catalytic activity of the mixed oxide, Fe–Ti-oxide

In an effort to point out the role of the Fe–Ti interaction in the catalytic activity, chlorobenzene oxidation was studied over Fe–Ti-oxide. Interestingly, this material showed significantly higher catalytic activity at 325°C than all other catalysts in study including the supported catalyst, $\text{Fe}_2\text{O}_3/\text{TiO}_2$. While the conversion declined to 30–60% over the supported and pure oxide catalysts, it was 95–100% for Fe–Ti-oxide during 100-pulse experiments as shown in Fig. 11. Besides the higher conversion, significantly less benzene and no CO were observed, indicating a stronger potential for deep oxidation. These results clearly indicate some type of Fe–Ti synergic interaction which improved the catalytic performance. As part of this effect, both metals acted as textural promoters leading to an enhanced resistance to sintering upon heating and reaction. The mixed oxide exhibited significantly higher and more stable surface area as compared with the other related catalysts. Table 1 presents the surface areas of the catalysts after calcinations at different temperatures as well as before and after reactions at 325°C . Besides the role of the high-surface area, the higher catalytic activity can be attributed to other characteristics of this material which may include the ease of reducibility and high defect concentration. To support these suggestions, more work is ongoing to investigate the microstructure characteristics of this catalyst and any correlation with the catalytic activity. The powder XRD analysis of the

catalyst after reactions showed no changes indicating reasonable stability of the catalyst, especially against chlorination.

3.6. Chlorine measurements

In all of the activity studies, the FTIR spectra showed no Cl-containing byproducts. Chlorine, which was measured by iodometric titration [15] was the only Cl-containing product. Although no HCl was detected as a product by the FTIR analysis, titration with NaOH revealed a significant concentration of H^+ in the KI solutions. The acid can result from the presence of excess Cl_2 according to the following known oxidation–reduction reactions [15]:



The total amounts of chlorine calculated from the titrations are presented in Table 2. Elevated reaction temperatures are, generally, associated with higher Cl recovery which, in part, explains the higher activity at these temperatures. This is due to the enhanced desorption of the adsorbed Cl atoms from the surface at higher temperatures, which regenerates surface active sites. On the other hand, less desorption of the adsorbed intermediates takes place at lower temperatures leading to accumulation of such species on the surface and hence poisoning of reactive sites. The high chlorine recovery associated with 100% conversion suggests that no chlorination of the catalysts takes place, which was also supported by the XRD analysis of the catalysts after reactions. This also means that the active phase does not contain any partially chlorinated oxide as was suggested for TiO_2 -supported manganese oxide in the literature [16].

3.7. The effect of water and mechanistic considerations

The effect of water on the catalytic activity of the Fe- and Ti-based catalysts was studied at 325°C by introducing water into the gas stream as pulses concurrently with chlorobenzene (1:2 chlorobenzene:water molar ratio). Water showed a negative effect on the catalytic activity of the supported as well as the mixed catalysts where the conversion decreased slightly compared with the corresponding activities in the absence of water. In other studies [4,17], water showed a positive effect on the dechlorination of aliphatic COCs which was proposed to be due to removal of adsorbed Cl atoms in the form of HCl, and to

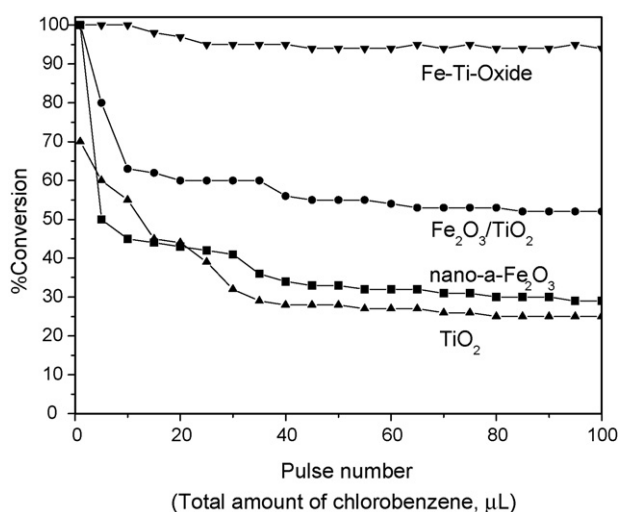


Fig. 11. The conversion of chlorobenzene over Fe–Ti-oxide at 325°C compared with the other related catalysts.

Table 2

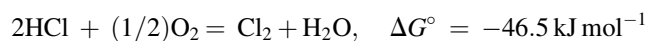
The amounts of chlorine from reactions at different temperatures as determined by iodometric and acid–base titrations

The catalyst ($^\circ\text{C}$)	Temperature	% Conversion ^a	% Cl recovery as Cl_2
$\text{Fe}_2\text{O}_3/\text{TiO}_2$	325	~60	55
Fe–Ti-oxide	325	~95	81
$\text{Fe}_2\text{O}_3/\text{TiO}_2$	400	100	95
Nano- α - Fe_2O_3	400	~50	46
TiO_2	400	~50	45

^a After steady-state conditions were achieved.

its role in increasing the Brönsted acid sites which were believed to be the active sites. In those studies, HCl was the main Cl-containing product, especially in the presence of water where its adsorption regenerated the surface Brönsted acid sites. It has also been reported that the effect of water, whether positive or negative, is dependent on its concentration [8,18]. Obviously, this is not the case in the oxidation of chlorobenzene in the current study as HCl was never observed as a product. For testing purposes only, the oxidation reaction of 1,2-dichloroethane was carried out over $\text{Fe}_2\text{O}_3/\text{TiO}_2$ under the same current conditions and HCl was observed as a major product in the FTIR spectra.

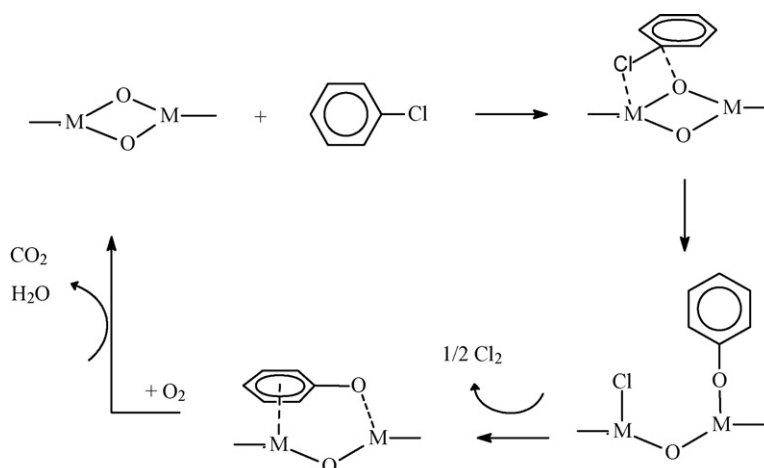
The negative effect of water and the absence of HCl as a product strongly suggest that the active sites for the chlorobenzene oxidation are not Brönsted acid sites. Instead, they are more likely to be Lewis acid–base sites. This explains the negative effect of water as the adsorption of water decreases the concentration of these sites. One may suggest that HCl may have formed and was catalytically converted to Cl_2 according to Deacon reaction [19]. It is known that both HCl and Cl_2 can be obtained because of the Deacon equilibrium:



However, the absence of HCl completely, even at high temperatures which are expected to shift the thermodynamic equilibrium of the Deacon reaction toward HCl formation, allows us to rule out this suggestion.

Therefore, it is very likely that the active sites are Lewis acid–base sites and the reaction pathway is similar to the known Mars van Krevelen mechanism. This mechanism generally involves dissociative adsorption on a metal oxide site, a change of oxidation state of the cations (redox process) and eventually insertion of lattice nucleophilic oxygen into the adsorbed molecule. Consequently, the first step is believed to be nucleophilic substitution resulting in dissociative adsorption via Cl abstraction by a Lewis acid site, and the formation of surface phenolates (Scheme 1). This is what one may expect as the polar C–Cl bond is the weakest in the molecule and is

expected to be cleaved first. The involvement of lattice oxygen resulted eventually in some oxidation to CO_2 as was evident from reactions in the absence of oxygen where some CO_2 was observed. This explains why MgO catalysts showed considerably lower activity as MgO is a very ionic oxide in which oxygen atoms are not as labile as in transition metal oxides. In addition, preliminary results from an FTIR study of the surface and adsorbed intermediates in the absence of oxygen showed that several partial oxidation intermediates, including phenolates and carboxylates, formed on the surface. These results strongly indicate the involvement of the lattice oxygen in the oxidation process supporting the proposed mechanism. These observations are also in agreement with similar results reported in the literature on the oxidation of chlorinated aromatics [5,8]. It is also expected that the activation of the aromatic ring be enhanced through interaction with surface metal sites via its π -electrons, especially after desorption of Cl atoms, as Cl_2 , from the surface. Finally, interaction with molecular oxygen regenerates the surface and results in the complete oxidation to CO_2 . Scheme 1 presents these suggestions as the main steps of the mechanism without accounting for the formation of benzene. A detailed mechanism will be elucidated from an ongoing FTIR study of the surface and surface intermediates which will be published separately. In conclusion we believe that the unusual formation of Cl_2 instead of HCl, as reported in the literature over other transition metal oxide-based catalysts, is most likely due to the nature of the initial adsorption step. The mechanism proposed in the literature is based on the adsorption of chlorobenzene on Brönsted acid sites which eventually resulted in HCl formation [20]. Therefore, the reactivity increased with upgrading the catalysts in a way that increased the number of surface Brönsted acid sites [21]. Similar mechanism was also proposed for the oxidation of chlorinated aliphatic hydrocarbons [22]. Obviously, when the Cl is adsorbed and is abstracted by a Brönsted acid site, HCl is expected to eliminate from the surface. On the other hand, if the Cl is abstracted by a Lewis acid site, as proposed in the current work, the reaction may proceed differently depending on other factors which probably affect the mechanism especially H/Cl



Scheme 1. Proposed main steps in the mechanism of the catalytic oxidation of chlorobenzene.

ratio in the adsorbed molecule and the Brönsted acidity of the surface.

Another factor that is also worth considering is the concentration of the chlorinated reagent in the gaseous stream. It is possible that the high concentration of chlorobenzene in our study, which is expected to result in lower Brönsted sites/Cl ratio, enhanced the formation of Cl_2 on the account of HCl. Future work on reactions under different concentrations can prove the feasibility of this suggestion.

4. Conclusions

High-surface area Fe–Ti-oxide was prepared via a simple sol–gel route. The supported, $\text{Fe}_2\text{O}_3/\text{TiO}_2$, and the mixed Fe–Ti-oxide catalysts showed significantly higher catalytic activities for the oxidation of chlorobenzene as compared with the corresponding pure oxides. Interestingly, the Fe–Ti-oxide catalyst exhibited the highest activity and showed a promising catalytic potential for the complete oxidation of chlorobenzene at relatively low temperatures, without the formation of any other chlorinated organics. Besides the role of iron oxide in the redox process, the high-surface area and the high affinity of Ti^{4+} sites to adsorb chlorobenzene are two important characteristics that contribute to the enhanced activity of the supported as well as the mixed oxide catalysts.

The Nature of the products and the negative effect of water on the catalytic activity allowed for drawing some conclusions in relation to the reaction mechanism. This mechanism is most likely similar to the known Mars van Krevelen mechanism, which is based on an oxidation–reduction process. The first step of the mechanism is dissociative adsorption of C–Cl on Lewis acid–base sites followed by lattice oxygen abstraction resulting in partial oxidation intermediates. Reaction with molecular oxygen from the gas phase eventually results in the complete oxidation and the regeneration of the surface. Chlorine was a major product on the account of HCl over the Fe–Ti-based catalysts. This unusual behavior, as compared with the literature, was explained based on the proposed mechanism, especially the adsorption step which takes place on Lewis acid sites. The high concentration of chlorobenzene in the gaseous stream may also have a role in the formation of Cl_2 as it

decreases the Brönsted acid sites to Cl ratio which decreases the chance for HCl formation.

Acknowledgement

This work was financially supported by the UAE University, Grant No. 04-03-2-11/05.

References

- [1] M. Taralunga, J. Mijoin, P. Magnoux, *Appl. Catal. B: Environ.* 60 (2005) 163–171.
- [2] E. Finocchio, G. Busca, M. Notaro, *Appl. Catal. B: Environ.* 62 (2006) 12.
- [3] S. Scire, S. Minico, C. Crisafulli, *Appl. Catal. B: Environ.* 45 (2003) 117–125.
- [4] D. Döbber, D. Kießling, W. Schmitz, G. Wendt, *Appl. Catal. B: Environ.* 52 (2004) 135–143.
- [5] J. Lichtenberger, M.D. Amiridis, *J. Catal.* 223 (2004) 296–308.
- [6] M.A. Larrubia, G. Busca, *Appl. Catal. B: Environ.* 39 (2002) 343–352.
- [7] L. Forni, I. Rossetti, *Appl. Catal. B: Environ.* 38 (2002) 29.
- [8] S. Krishnamoorthy, J.A. Rivas, M. Amiridis, *J. Catal.* 193 (2000) 264–272.
- [9] A.M. Padilla, J. Corella, J.M. Toledo, *Appl. Catal. B: Environ.* 22 (1999) 107–121.
- [10] H. Itoh, S. Utamapanya, J.V. Stark, K.J. Klabunde, *Chem. Mater.* 15 (1993) 71–77.
- [11] K.J. Klabunde, A. Khaleel, D. Park, *High Temp. Mater. Sci.* 33 (1995) 99–106.
- [12] I.E. Grey, C. Li, J.A. Watts, *Am. Miner.* 68 (1983) 981–988.
- [13] A. Khaleel, *Chem. Eur. J.* 10 (2004) 925–932.
- [14] F. Bertinchamps, C. Grégoire, E.M. Gaigneaux, *Appl. Catal. B: Environ.* 66 (2006) 1–9.
- [15] G. Svehla, *Qualitative Inorganic Analysis*, 6th ed., Longman Scientific and Technical, Essex, England, 1987, p. 179.
- [16] Y. Liu, M. Luo, Z. Wei, Q. Xin, P. Ying, C. Li, *Appl. Catal. B: Environ.* 29 (2001) 61–67.
- [17] A. Khaleel, *Micropor. Mesopor. Mater.* 91 (2006) 53–58.
- [18] F. Bertinchamps, A. Attianese, M.M. Mestdagh, E.M. Gaigneaux, *Catal. Today* 112 (2006) 165–168.
- [19] G. Sinquin, C. Petit, S. Libs, J.P. Hindermann, A. Kiennemann, *Appl. Catal. B: Environ.* 27 (2000) 105–115.
- [20] F. Bertinchamps, C. Grégoire, E.M. Gaigneaux, *Appl. Catal. B: Environ.* 66 (2006) 10–22.
- [21] D.P. Debecker, F. Bertinchamps, N. Blangenois, P. Eloy, E.M. Gaigneaux, *Appl. Catal. B: Environ.* 74 (2007) 223–232.
- [22] R. van den Brink, P. Mulder, R. Louw, G. Sinquin, C. Petit, J.-P. Hindermann, *J. Catal.* 180 (1998) 153–160.